Material Mismatch Effect on the Fracture of a Bone-Composite Cement Interface

M. Khandaker[1*], S. Tarantini[2]
Department of Engineering and Physics, University of Central Oklahoma, Edmond, Oklahoma, USA
Email: *[1]mkhandaker@uco.edu; [2]starantini@uco.edu

***Abstract*- The interfacial mechanics at the bone-implant interface is a critical issue for implant fixation and the filling of bone defects created by tumors and/or their excision. Our previous study found that micron and nano sizes MgO particles improved the fracture toughness of bone-cement interfaces under tension loading. The strength of bonding of different types of bone with different types of implants may not be the same. The aims of this research were to determine the influences of material mismatch due to bone orientation and a magnesium oxide (MgO) filler material for PMMA bone cement on the mechanical strength between bone and bone cement specimens. This research studied the longitudinal and transverse directions bovine cortical bone as different bone materials and poly Methyl MethAcrylate (PMMA) bone cement with and without MgO additives as different implant materials. The scope of work for this study was: (1) to determine the bending strength and modulus of different bone and bone cement specimens, (2) to determine whether inclusion of MgO particles on PMMA has any influence on these mechanical properties of PMMA, and (3) to determine whether bone orientation and inclusion of MgO particles with PMMA has any influence on the interface strength between bone and PMMA. This study showed that bone orientation has statistically significant effect on the bonding strength between bone and bone cement specimens (P value<0.05). This study also found that while MgO additive decreased the bending strength and modulus of PMMA bone cement, but the inclusion of MgO additives with PMMA bone cement has no statistically significant effect on the bonding strength between bone and bone cement specimens (P value>0.05).**

Keywords- Cortical Bone; PMMA; Mgo; Additives; Mechanical Properties

I. INTRODUCTION

Bone is composed of two bony phases, cortical and cancellous. Cortical bone, also known as compact bone, is a dense, solid mass with microscopic channels called haversian canals. Cancellous bone, also known as trabecular bone, is a soft spongy like substance in the center of the bone. Cortical bone is a very complex matrix of collagen fibers and crystallized minerals. The orientation of osteons and haversian canals make cortical bone a non-homogenous and anisotropic material. According to orientation of the osteons, researchers classified cortical bone test specimen in two categories: longitudinal and transverse [1]. Damage and failure of these bones have already been studied in quasi-static tensile and dynamic loads. Large variations of stress failure were reported by the researchers due to variability of test methods, test types, loading rate, geometry, orientation, age, location, species, test temperature, and preservation techniques [2].

Various kinds of polymeric implant materials are used for the filling of bone defects created by tumors and/or their excision as well as for the joining of fractured bony elements. The implant-bone interface is crucial to the stability of the implanted components. The mechanical properties of bone and implant materials at the interface under load-bearing condition have significant influence on the quality of bone/implant union. Polymers used in orthopedic implants can be grouped into two families: long term implantable and bioresorbable [3]. Long term implantable polymers commonly include PMMA, polyethylene, urethane, and polyketone. They provide "permanent" structural support within the body in the form of sutures, fabric mesh, tubing, bone screws and anchors, or complete bone replacements. The strength of bonding of longitudinal and transverse direction cortical bone with implant materials during orthopedic surgery applications may not be the same [4]. The differences of the failure characteristics of between longitudinal bone (LB)-implant and transverse bone (TB)-implant interfaces under loading condition are not fully understood. In the present study, the bonding stress of LB/bone cement and TB/bone cement was evaluated to investigate the effect of orientation of bone on bonding stress between bone and bone cement. The first aim of this research was to determine whether bone orientation of bone has any influence on the bonding strength between bone and PMMA cement.

The most challenging issue associated with commercially available polymer is their poor osseointegration (incorporation of the cement with surrounding bone tissues) [5]. Problems about infection and loosening of the bone cements at the bone-cement interface have been reported in Literature [6]. Our previous studies found that the osteoblast cell adhesion with micron and nano sizes MgO particles incorporated PMMA cement was higher compared to the osteoblast cell adhesion with PMMA cement only [7]. Such osseo-integrated cells can eliminate contact between the bone and the environment and restricting contamination at the cemented prosthetic joint. Another way to reduce loosening would be to increase mechanical interlock between bone and cement [8, 9]. This can be done by enhancing the surface roughness of the PMMA cement. Several research groups found improvement of PMMA bone cements surface roughness properties by incorporating different kinds of additives materials with the PMMA cement [6, 10-13]. Our previous study found that micron and nano sizes MgO particles improved the fracture toughness of bone-cement interfaces

under tension loading [14]. The strength of bonding of bone with these additives incorporated PMMA bone cement may be different from bonding of bone with PMMA without these additives. The influences of the inclusion of these additives with bone cement on the bonding stress between natural bone and cements were not investigated yet. Such study is required for the suitability of using the additives with the bone cement. Ricker *et al*. [13] research on PMMA cement showed increased surface roughness, and enhanced cell adhesion of mouse osteoblast cell on PMMA due to the inclusion of MgO additives with PMMA. The suitability of incorporating MgO additive with bone cement requires complete understanding of the failure characteristics of bone/MgO additives incorporated bone cement interfaces. No study has been conducted to evaluate the effect of MgO additives on the mechanical integrity between bone and PMMA cement with MgO additives. In this present study, two kinds of bone cement were investigated. Cobalt™ HV bone cement (referred in this literature as CBC), a commercial orthopedic bone cement, was used as control PMMA bone cement. Cobalt™ HV bone cement with 36 μm mesh size MgO particle (referred in this literature as mCBC), was used as an alternative PMMA based bone cement. The second aim of this research was to determine whether inclusion of MgO particles with PMMA bone cement has any influence on the bonding strength between bone and PMMA cement.

The present study is based on the hypothesis that the material mismatch at bone/ bone cement interface due to bone orientation and additive materials for bone cement may have significant influence on the quality of bone/bone cement union. The scope of works for this research were: (1) to quantify elastic and fracture properties of different bone and bone cement specimens, (2) to determine whether inclusion of MgO additives with PMMA has any influence on the mechanical properties of CBC, and (3) to determine whether bone orientation and inclusion of MgO particles with PMMA has any influence on the interface strength between bone and CBC. A custom made three-point bend test setup was designed and fabricated. Two groups of specimens were prepared: homogenous (LB, TB, CBC, mCBC) and bimaterial specimens (LB-CBC, LB-mCBC, TB-CBC, and TB-mCBC). ASTM 399 standard three-point bend (3PB) tests were conducted on the first group of specimens to quantify the elastic and fracture properties differences between natural bones and cements specimens. Three-point bend (3PB) tests were conducted on the bimaterial specimens to quantify the bone orientation and MgO additive material effects on the bonding strength of the corresponding specimens.

II. MATERIALS AND METHODS

A. Design and instrumentation of the setup

The complete test setup is shown in Figure 1(a). The instrumentation of the setup includes high precision nanoscale microactuator (Newport™ LTA-HL® actuator) with motion controller (SMC 100), 50 lb load cell (Futek™ LCM300, model number FSH02630) with sensor (Futek™ IPM500), microscope (Nikon SMZ 1000 streomicroscope). All instruments were calibrated before testing. The 3PB bend stage consists of base, stage-base connector, sliding bar, indenter, and specimen holder. An optical xyz stage was assembled with the base for microscopic viewing purposes using stage-base connector. Actuator was mounted on the base to push the sliding bar. The other side of the sliding bar was fastened with the loadcell. Two high quality smooth aluminum rods were used to transfer actuator linear motion to the sliding bar. The other end of the loadcell was connected to the round edge indenter. Concave endmills $^{1}/_{32}$" radius was used to create the round edge in the indenter. The specimen holder was fastened to the base to hold the 3PB specimen on the top of two high strength steel rollers. The distance between the rollers was 16 mm to maintain ASTM E399 3PB support to the specimen. A micrometer with a sharp edge needle was attached at the side of the base. The purpose of the micrometer was to align the center of the notch of the specimen and the center of the indenter with the help of the microscope. A mold was designed and fabricated for the preparation of bone-cement specimen using dimension elite 3D printer (Figure 1(b)). The mold was made of tough ABS plastic. Glass slides were glued at the interior boundaries of the mold to avoid contact of PMMA with ABS plastic during curing.

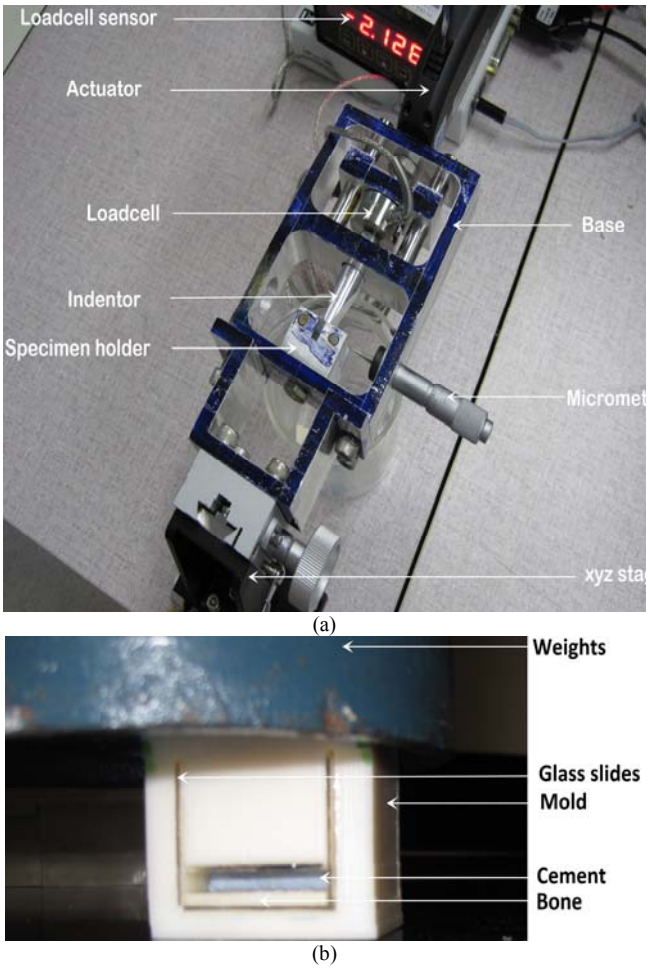

Fig. 1 (a) The experimental setup and (b) Mold for the preparation of bone-cement specimens

B. Sample Preparation

Since density had a large influence on failure process, therefore, in this study small ASTM 399 standard specimens were prepared to get low density variation homogenous specimen [15]. Two groups of rectangular, without and with single edge notch at the center of the specimen, cortical bone specimen were prepared in this study to evaluate elastic and fracture properties respectively. Bone samples were extracted from the mid-diaphyses of fresh bovine femoral shaft obtained from a local abattoir. The femoral shafts were cut longitudinally into two blocks. Each block was milled down to a thickness of 2 mm as shown in Figure 2. Bone coupons of (20×40~50×2) mm dimension were prepared from each block. The bone coupons was cut further longitudinally and transversely to create (20×4×2) mm LB and TB three-point bend bone samples, respectively. Buehler low-speed saw cutter (isomet 11-1180-100) was used to cut the samples from the coupons. A center notch was created using the saw cutter on each of the longitudinal cracking (referred in the literature as CL specimen) and transverse cracking (referred in the literature as LC) specimen. Figure 2 illustrates the different kinds of bone samples prepared during this study.

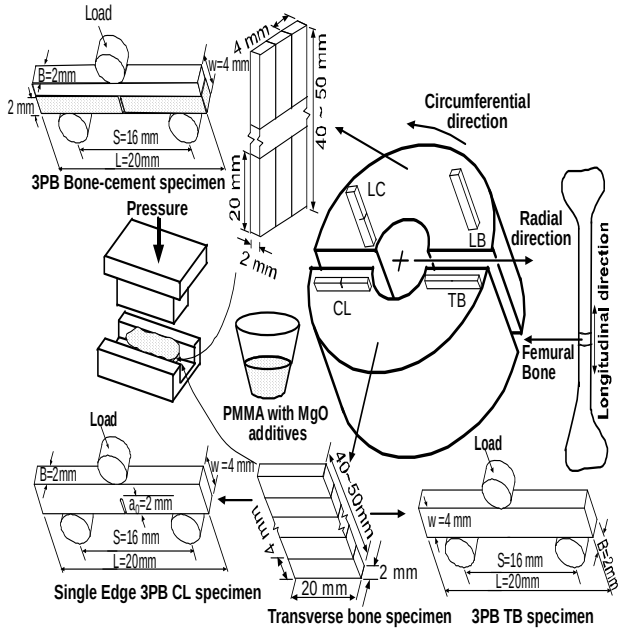

Fig. 2 Schematic views of the specimen preparation protocols, specimen dimension, orientation and loading direction for the three point bend and fracture tests.

For the bend specimen, specimen is named according to the orientation of osteon in the bone specimen., the long axis is parallel to osteon direction in LB, whereas the long axis is transvers to osteon direction in TB. For the single edge notch bend specimen, the 1st letter in the specimen designation refers to the normal direction to the crack plane, while the 2nd letter refers to the expected direction for crack propagation.

Two groups of bone cement were used for preparing cements (CBC and mCBC). Also four groups of bone/bone cement interface specimen were prepared based on the bone and cement types. They are reffered in the literature as LB/CBC, TB/CBC, LB/mCBC, and TB/mCBC specimens. According to the manufacturer recommendation (Biomet, Inc), 10 grams of poly Methyl MethAcrylate (PMMA) beads were added to 5 ml of benzoyl peroxide monomer to prepare the CBC specimen. In order to create mCBC specimens, 10 percent (w/w) of the 36 μm mesh size MgO additives powders (0.5 gm) were mixed with the PMMA (4.5 gm) and added to the monomer (5 ml). LB/cement and TB/cement were prepared from the same femoral bone. The coupons were cut into (20×10×2) dimension samples for the bone/cement specimens as shown in Figure 2. A glass mold was used to prepare different kinds of (20×60×4) mm cement and bone-cement blocks. To prepare the different cement specimens, the cement was added to the top half of the glass molding chamber while the cement was in its doughy phase. In order to prepare the different bone/bone cement interface specimens, the (20×10×2) dimension bone blocks were placed in the mold first, and then cement was poured on top of it. A set of weights equivalent to 80 kPa pressure (clinically applied range [16]) were applied to the samples during the curing process. The pressure was initiated at exactly three minutes after the onset of mixing and was sustained throughout the curing period [17]. After curing, the blocks were carefully secured in the double sided chuck of the Buehler isomet low speed cutter. The block was cut into (20×4×2) mm size pieces using the Buehler. The center notches for SENB homogeneous and bimaterial specimens were prepared using a $3\times0.006\times{}^{1}/_{2}$ in. wafering blade. During the specimen preparation procedures, the bone was always kept moist with a saline solution. The schematic view and dimension of the prepared specimen are represented in Figure 2.

C. Experiment

Three-point bend (3PB) tests were conducted on homogeneous and bimaterial specimens at room temperature using the 3PB stage. The specimens were mounted on the 3PB holder in the test stage. Nikon SMZ 1000 steromicroscope was used to align the center of the specimen and the center of indenter round edge. All specimens were loaded using round edge indenter with a loading rate equal to 0.001 mm/s using precision linear actuator. The load and displacement were continuously recorded until the failure of the specimens. During the testing, the wet bone and bone-cement samples were continuously kept moist using deionized water, as saline was too corrosive for the specimen holder.

D. Data Analysis

Several biomechanical parameters were derived from the 3PB tests to compare the material properties between bone and cements. The value of Young's modulus, E for a three-point bend specimen was calculated using [2]: $E=kS^3/4BW^3$, where k is the stiffness of the specimen as measured by the slope of the load-deflection curve at the elastic region. Bending strength, σ_f, was calculated using [2]: $\sigma_f=3P_{max}S/2BW^2$, where P_{max} is the ultimate load (force at failure), S is the standard loading span for the 3PB specimen, B is the thickness, and W is the width of the specimen. For

the SENB test, the maximum load, P_{max}, at the onset of crack extension from the notch tip was used to calculate the fracture toughness, K_I using relationship [18]: $K_I=P_{max}Sf(\alpha)/BW^{3/2}$, where α is the normalized initial crack length ($\alpha=a/W$) and $f(\alpha)$ is a dimensionless geometric function. The following equation can be used to calculate $f(\alpha)$ [18].

$$f(\alpha)=\frac{3(\alpha)^{1/2}\left[1.99-(\alpha)(1-\alpha)\times\left(2.15-3.93\alpha+2.7(\alpha)^2\right)\right]}{2(1+2(\alpha))(1-\alpha)^{3/2}} \quad (1)$$

Interfacial fracture toughness for a bi-material specimen was calculated using the equation by Lucksanasombool *et al.* [19],

$$G_{IC}=\frac{M^2\left(1-\nu_2^2\right)}{2E_2}\left(\frac{1}{I_2}-\frac{\lambda}{I_C}\right) \quad (2)$$

where the Subscript 2 refers to the properties of the unnotched layer (LB or TB), and the subscript *c* refers the property of the cement layer (CBC or mCBC). In Eq. (2), $\lambda=E_2(1-\nu_1^2)/E_1(1-\nu_2^2)$, where Subscript 1 refers to the properties of the notched cement layer, M is the maximum moment corresponding to interface crack initiation at the crack tip due to 3PB loading ($M=P_{max}S/4$), and I_C ($I_c=bh_1^3/12+\lambda bh_2^3/12+b\lambda h_1h_2\,(h_1+h_2)^2/4(h_1+\lambda h_2)$ is the moment of inertia for the cement layer only, where h_1 and h_2 is the height of each layer. I_2 ($I_2=bh_2^3/12$) is the moment of inertia of the bone layer. Eq. (2) considers the through-thickness crack occurring in the center of the beam and the length of the interfacial crack propagate symmetrically from the center is zero.

E. Statistical Analysis

Statistical analyses were performed using Student's t-test for the mechanical properties between specimens using Microsoft Excel 2000 statistical analysis toolkit. Data sets with a p-value <0.05 were considered significantly different.

III. RESULTS

Table Ⅰ shows the statistic of experimental parameters found from the 3PB flexural and fracture tests. Figure 3(a) compares the 3PB load-displacement curves of a longitudinal bone (LB), transverse bone (TB), CBC, and mCBC specimens. The characteristics of load-displacement curve of the bone specimens were different from the various cement specimens. Figure 3 (b) presents the bending modulus of TB specimen (6.84 ± 0.12 GPa) is significantly higher than stiffness of LB specimen (5.04 ± 0.44 GPa). The modulus of both LB and TB specimen were higher than CBC (1.07 ± .04GPa) and mCBC specimens (0.85 ± 0.06 GPa). We have found a statistically significant difference of modulus between CBC and mCBC specimens (P value < 0.01). Ductility (ultimate displacement) of CBC specimens was higher than LB, TB and mCBC specimens. Figure 3 (b) illustrates a comparison of average bending modulus of different kinds of bone and cement specimens. Table 1 shows the bending strength of TB samples was significantly higher compared to the transverse and CBC specimens (P value < 0.01). The bending strength of CBC specimens was significantly higher than mCBC specimens (P value < 0.01).

TABLE Ⅰ DESCRIPTIVE STATISTICS OF THE EXPERIMENTAL PARAMETERS FOUND IN THIS STUDY. DATA IS REPRESENTED AS MEAN ± STANDARD DEVIATION (NO OF SAMPLES)

Mechanical Properties	***Specimen Types***			
	Single Material Specimen			
	TB	***LB***	***CBC***	***mCBC***
Bending modulus (GPa)	5.04 ± 0.44 (9)	6.84 ± 0.12 (10)	1.07 ± 0.04 (5)	0.85 ± 0.06 (5)
Bending strength (MPa)	64.83 ± 4.58 (9)	191 ± 20.02 (10)	67.84 ± 6.95 (5)	60.52 ± 1.31 (5)
	Bi-material Specimen			
	TB-CBC	LB-CBC	TB-mCBC	LB-mCBC
Fracture toughness (kJ/m^2)	0.73 ±.045 (4)	2.03 ± 0.25 (2)	1.15 ± 0.22 (3)	2.24 ± 0.18 (2)

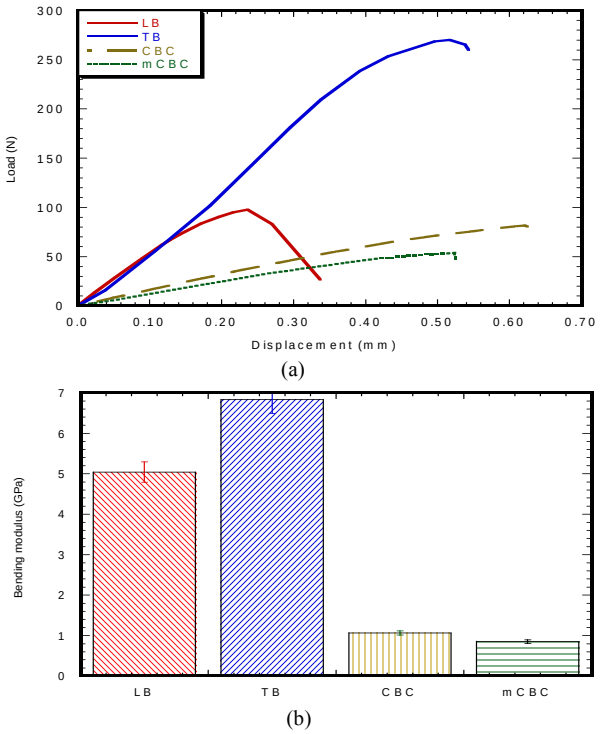

Fig. 3 (a) Typical applied load versus the load point displacement plot of a LB, TB, CBC and mCBC specimens (b) variation of interface fracture toughness of different kinds of the bimaterial specimens..

Figure 4(a) compares the load-displacement curves of a SENB bone specimen (CL and LC) with SENB cement specimen (CBC and mCBC). The load-displacement characteristics of CL and LC specimens were different from CBC and mCBC cement specimens. In case of bone specimen, load-displacement curve shows initially an elastic (linear response) region, followed by a short broad inelastic region, and then catastrophic failure, whereas all CBC specimens exhibited a long elastic and inelastic region before catastrophic failure. The total deformation before the commencement of failure for the CBC specimens was higher than CL, LC, and mCBC specimens. The initial slope of the load-displacement curve for LC specimen was higher than those of CL, CBC, and mCBC specimens. The

load-displacement behavior demonstrated that the cement specimens failed in a more stable manner than those of bone specimen after reaching the maximum load. The Mode I crack tip fracture toughness, K_{IC}, for each specimen was calculated from the maximum load value at which the load-displacement curve deviates from linearity. Figure 4 (b) shows fracture toughness of different bone and cement specimens. This figure demonstrates that the K_{IC} values of LC specimen were significantly higher than the K_{IC} values of CL, CBC, and mCBC specimens (P value < 0.01).

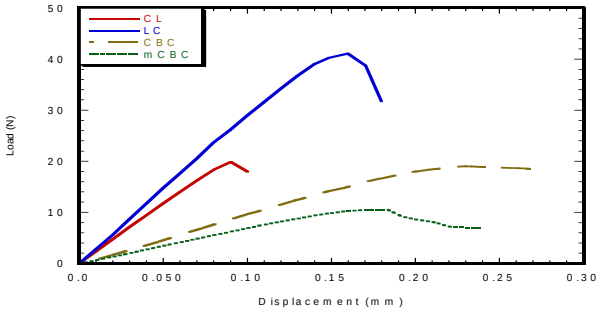

(a)

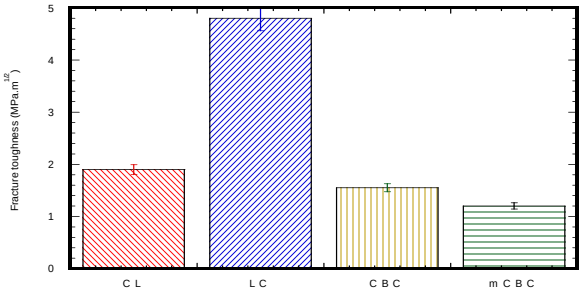

(b)

Fig. 4 Three-point SENB test results of five homogenous specimens: (a) fracture toughness; and (b) work of fracture.

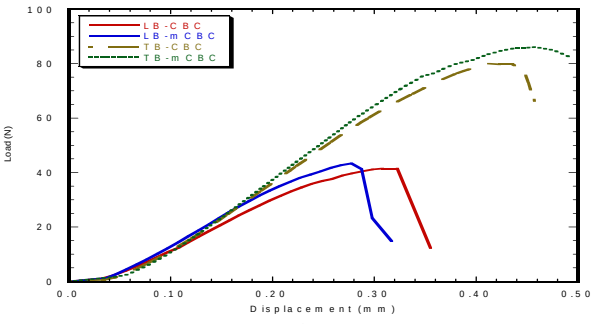

(a)

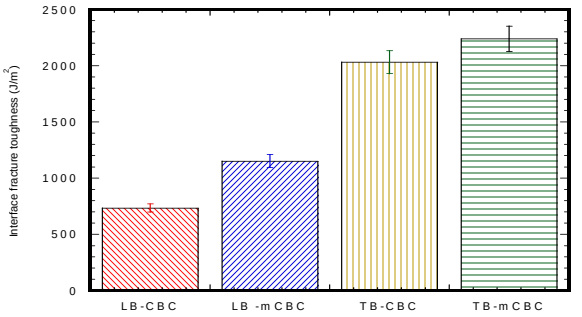

(b)

Fig. 5 (a) Typical load versus the load point displacement for different kinds of the bimaterial specimens (b) variation of interface fracture toughness of different kinds of the bimaterial specimens.

Figure 5(a) compares the SENB load-displacement curves of bimaterial specimens (LB/CBC, TB/CBC, LB/mCBC, and TB/mCBC). The load-displacement response of longitudinal bimaterial specimens is characterized as initially elastic response, followed by a short inelastic region and then a sudden descending response. On the other hand, the load-displacement response of transverse bimaterial specimens is characterized as having higher initially elastic response, broader inelastic region, and smoother descending response of load-displacement compared to those of longitudinal bimaterial specimens. The characteristics of the load-displacement curves of MgO included bi-material specimen were not different from those of bi-material specimen without MgO additive. The interface fracture toughness, G_{IC}, for each specimen was calculated from the maximum load value at which the load-displacement curve deviates from linearity. Figure 5(b) compares the average interface fracture toughness values calculated using Eq. (2). The difference of the interface fracture toughness between LB/CBC and LB/mCBC was not statistically significant (p value 0.12). Also, the difference of the interface fracture toughness between TB/CBC and TB/mCBC specimens was not statistically significant (p value 0.58). In contrast, the difference of the interface fracture toughness between LB/CBC and TB/CBC was statistically significant (p value 0.12). The difference of the interface fracture toughness between LB/mCBC and TB/mCBC specimens was statistically significant (p value 0.03). The above statistical analysis on the G_{IC} data confirms no significant difference of the G_{IC} of bone/cement samples due to the addition of MgO (P values>0.05), whereas significant difference of the G_{IC} of bone/cement samples due to the orientation of bone (P values<0.05).

IV. DISCUSSION

Ultimate load, modulus, work to failure (area under the load-displacement curve), and ultimate displacement parameters of a load-displacement curve in a 3PB test reflect the general integrity, mineralization, amount of energy before break and brittleness of the tested specimens, respectively [2]. Figure 3 demonstrated a clear difference of these properties between natural bone and cement specimens. Comparing these properties for different kinds of cement specimens, improved brittleness of cement was found due to the inclusion of MgO additives to CBC. However, no noticeable improvement of integrity, mineralization, and amount of energy before breaking for CBC specimen due to the inclusion of MgO additives to CBC was found. The values of the bending strength of mCBC were lower compared to CBC due to the differences of structures between CBC and mCBC as shown in Figure 6. The MgO particles made it difficult for the PMMA beads to mix uniformly with the MMA monomer. It creates volume defects, which are the weak points in the cement. The weak points in the cement lead to stress concentration under external loading [20]. Inclusion of MgO additives to CBC reduces its elastic properties compare to CBC due to the fact that particles with higher molecular weight (MW) like PMMA dissolves in monomer slower than lower MW particles like MgO (M_W = 40.3, provided by the

manufacturer). This decreases the amount of monomer available for the cross linking with the PMMA during mixing, which leads to more defects in the mCBC specimens. Scanning microscopic images of grounded-polished CBC cement specimens shows the defects (Fig. 6).

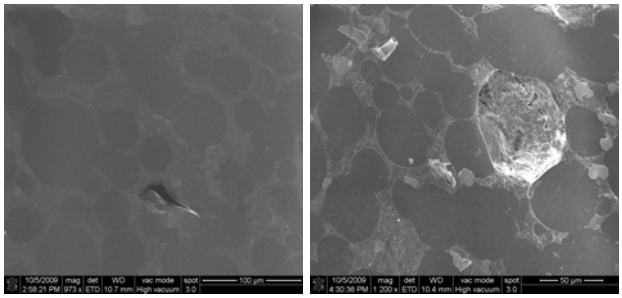

(a) (b)

Fig. 6 Scanning electron microscopy images of grinded-polished CBC specimens: (a) CBC only and (b) CBC with 36 μm MgO additives

The non-catastrophic failure behavior of the CBC and mCBC specimens (Figure 4(a)) indicates the presence of stress shielding mechanism. The values of the fracture strength of CBC were lower comparing to natural bone because of the difference of stress shielding mechanism between CBC and bone materials under loading. Cortical bone is made of apatite and fibers of collagen. Longitudinal and transverse cracking cortical bone has various mechanism of shielding itself from crack propagation under loading. The mechanism include crack bridging and microcracking [21]. On the other hand, fracture originates at the grain boundary of the CBC and mCBC polymeric matrix and propagates along the boundary of the polymeric matrix as shown in Figure 7(a, b). Addition of MgO additives particles to CBC, make the grain boundary weaker, which leads to lower fracture toughness for mCBC comparing to CBC samples. Chan research group [22] also reported similar stress shielding behavior for bioactive composite cement (bis-GMA based monomer blend) with addition of Schott glass and SiO_2 nanoparticles. Stress shielding mechanism, like particle bridging, debonding at the poles of particle/matrix interface, crack trapping, and crack deflection around the particles, were identified as the cause for this improved fracture toughness.

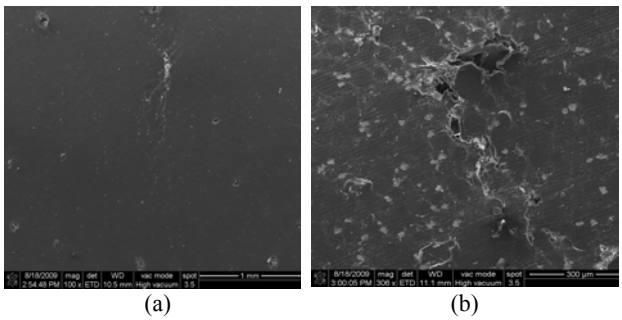

(a) (b)

Fig.7 Scanning electron microscopy images of fractured specimen: (a) CBC and (b) mCBC

One of the aims in this study was to investigate and quantify the effects of bone orientation on the mechanical integrity of the bone-cement interfaces. This study revealed significant differences of elastic and fracture strength between LB-CBC and TB-CBC specimens. In addition, this study found that the bonding strength of TB with CBC cements was higher than the bonding strength of LB with CBC cements. This orientation effect on the interface fracture strength of the LB/cement and TB/cement specimens is related to the surface roughness difference between bone and cement. The energy required for the propagation of interface crack normal to the osteon for TB-cement sample can be more than the energy requirement for the crack propagation parallel to the wall of the osteon for LB-cement samples. All samples (LB or TB) were prepared with Isomet, however, since bone is transversely isotropic, the surface roughness of LB may vary from TB.

Another aim of this study was to evaluate the effects of MgO additives on the mechanical integrity of the bone-cement interfaces. This study didn't find any statistically significant improvement due to inclusion of MgO on the bonding stress of longitudinal bone-mCBC specimen and transverse bone-mCBC specimen in comparison to longitudinal bone-CBC specimen and transverse bone-CBC specimen, respectively. One possible explanation for this phenomenon may be the residual stresses developed due to the setting reaction shrinkage and hygroscopic expansion when the mCBC is soaked with water during sample preparation. The volume of cured mCBC samples were reduced almost 2 times comparing to CBC without MgO additive during sample preparation. Such rapid shrinkage and expansion cause change of dimension at the interface of bone-mCBC specimen and create poor mechanical interlock between bone and mCBC.

The values of flexural and fracture properties of LB and TB in this study are in close agreement with Athanasiou *et al*. [23] and Lucksanasombool *et al*. [18]. There are no publications on the flexural and fracture properties of CBC as well as interfacial fracture toughness of bone-CBC to compare our results. However, the value of the flexural strength of CBC (67.84 ± 6.95 MPa) in this study is in close agreement with flexural strength of Palacos ® R bone cement (68 MPa) by Tunney *et al*. [24]. The value of the fracture toughness of CBC (1.55 ± 0.21MPa.$m^{1/2}$) in this study is in close agreement with fracture toughness of DePay CMW1 bone cement (1.44 ± 0.09 MPa.$m^{1/2}$) by Mousa *et al* [20]. The value of G_{IC} of bone - CBC interface in this study was significantly higher than Lucksanasombool *et al* [19] reported G_{IC} between bovine cortical bone and glass ionomer cement (FUJI II). This difference was reasonable since the cement and test method used in this study is different from the test specimen used by Lucksanasombool *et al*. [19].

Since these studies' goals were to determine the effect of MgO on the adhesion strength between bone-CBC specimens comparing to bone-CBC with MgO additive, the study was limited to preparing mCBC specimen with 10 wt% 36μm MgO, 1ml benzoyl peroxide for 2gm PMMA powder, and 80 kPa curing pressure. Further studies are required to investigate the effect of MgO particle size, monomer contents, and curing pressure on the bonding strength between bone and CBC with MgO additive specimen compare to the bonding strength between bone and CBC specimens without MgO additives.

V. CONCLUSION

The original aspects of this work are the effects of bone orientation and MgO additives on the mechanical strength of bone/cement union. The conclusions of this research are as follows: (1) inclusion of 10% (w/w) MgO particles in commercial Cobalt™ HV orthopedic bone cement (CBC) have decreased the elastic and fracture properties of CBC (*P* value <0.05); (2) the orientation of the bone has significant influence on the bonding strength between bone and cements; and (3) inclusion of MgO additives on CBC has no significant influence on the bonding strength between bone and CBC. Two important findings arose from this study which can benefit clinicians and biomedical bone cement researchers. Firstly, a higher bonding strength can be achieved between transverse bone and implant compare with longitudinal bone and implant during orthopedic surgery. Secondly, MgO microparticle additive can negatively affect the mechanical properties of PMMA cement. This detrimental effect of addition of microparticle additives into PMMA cement on the bonding strength between bone and bone cement could supersede the chemical and biological benefits achieved through the inclusion of additive materials to PMMA. Therefore, it could adversely affect the longevity of the cemented prosthetic joint.

ACKNOWLEDGEMENTS

This publication was made possible by Grant Number P2PRR016478 from the National Center for Research Resources, a component of National Institute of Health (NIH) and on campus grants from University of Central Oklahoma.

REFERENCES

[1] J. D. Currey, *Bones: Structure and Mechanics*: Princeton University Press, 2002.

[2] S. C. Cowin, *Bone Mechanics Handbook*, Second ed., 2001.

[3] S. Dumitriu, *Polymeric Biomaterials*: CRC Press, 2001.

[4] G. X. Ni, Y. S. Choy, W. W. Lu, A. H. W. Ngan, K. Y. Chiu, Z. Y. Li*, et al.*, "Nano-mechanics of bone and bioactive bone cement interfaces in a load-bearing model," *Biomaterials,* vol. 27, pp. 1963-1970, 2006.

[5] J. E. Barralet, K. J. Lilley, L. M. Grover, D. F. Farrar, C. Ansell, and U. Gbureck, "Cements from nanocrystalline hydroxyapatite," *Journal of Materials Science: Materials in Medicine,* vol. 15, pp. 407-411, 2004.

[6] G. Lewis, "Alternative acrylic bone cement formulations for cemented arthroplasties: Present status, key issues, and future prospects," *Journal of Biomedical Materials Research - Part B Applied Biomaterials,* vol. 84, pp. 301-319, 2008.

[7] M. Khandaker, Y. Li , P. Liu, and M. Vaughan, "Bioactive additives and functional monomers affect on PMMA bone cement: Mechanical and biocompatibility properties," in *2011 ASME International Mechanical Engineering Congress and Exposition*, Denver, Colorado, 2011.

[8] K. A. Mann, A. A. Edidin, N. R. Ordway, and M. T. Manley, "Fracture toughness of CoCr alloy-PMMA cement interfaces," *J. Biomed Mater. Res. (Applied Biomaterials),* vol. 38, pp. 211-219, 1997.

[9] K. L. Ohashi, A. C. Romero, P. D. McGowan, and M. T. Maloney, "Adhesion and reliablity of interfaces in cemented total joint arthroplasties," *Journal of orthopedic research,* vol. 16, pp. 705-714, 1998.

[10] H. Liu and T. J. Webster, "Nanomedicine for implants: A review of studies and necessary experimental tools," *Biomaterials,* vol. 28, pp. 354-369, 01/10/ 2007.

[11] S. J. Heo, S. A. Park, H. J. Shin, Y. J. Lee, T. R. Yoon, H. Y. Seo*, et al.*, "Evaluation of bonding stress for the newly suggested bone cement: comparison with currently used PMMA through animal studies," *Key Engineering Materials,* vol. 342-342, pp. 373-6, 2007.

[12] D. Khang, S. Y. Kim, P. Liu-Snyder, G. T. R. Palmore, S. M. Durbin, and T. J. Webster, "Enhanced fibronectin adsorption on carbon nanotube/poly(carbonate) urethane: Independent role of surface nano-roughness and associated surface energy," *Biomaterials,* vol. 28, pp. 4756-4768, 11/10/ 2007.

[13] A. Ricker, P. Liu-Snyder, and T. J. Webster, "The influence of nano MgO and BaSO4 particle size additives on properties of PMMA bone cement," *International Journal of Nanomedicine,* vol. 3, pp. 125-1, 2008.

[14] M. Khandaker, Y. Li , and T. Morris, "MgO micro/nano particles for the improvement of cement–bone interface," *Accepted in journal of biomechanics,* December 12 2012.

[15] M. Pithioux, D. Subit, and P. Chabrand, "Comparison of compact bone failure under two different loading rates: experimental and modelling approaches," *Medical Engineering & Physics,* vol. 26, pp. 647-653, Oct 2004.

[16] M. D. Ries, L. A. Rauscher, S. Hoskins, D. Lott, J. A. Richman, and F. Lynch, "Intramedullary pressure and pulmonary function during total knee arthroplasty," *Clinical Orthopaedics and Related Research,* pp. 154-160, 1998.

[17] J. Graham, M. Ries, and L. Pruitt, "Effect of bone porosity on the mechanical integrity of the bone-cement interface," *Journal of Bone and Joint Surgery-American Volume,* vol. 85A, pp. 1901-1908, Oct 2003.

[18] P. Lucksanasombool, W. A. J. Higgs, R. Higgs, and M. V. Swain, "Fracture toughness of bovine bone: influence of orientation and storage media," *Biomaterials,* vol. 22, pp. 3127-3132, Dec 2001.

[19] P. Lucksanasombool, W. A. J. Higgs, R. Higgs, and M. V. Swain, "Interfacial fracture toughness between bovine cortical bone and cements," *Biomaterials,* vol. 24, pp. 1159-1166, Mar 2003.

[20] W. F. Mousa, M. Kobayashi, S. Shinzato, M. Kamimura, M. Neo, S. Yoshihara*, et al.*, "Biological and mechanical properties of PMMA-based bioactive bone cements," *Biomaterials,* vol. 21, pp. 2137-2146, 2000.

[21] R. K. Nalla, J. H. Kinney, and R. O. Ritchie, "On the fracture of human dentin: Is it stress- or strain-controlled?," *Journal of Biomedical Materials Research Part A,* vol. 67A, pp. 484-495, Nov 1 2003.

[22] K. S. Chan, Y. D. Lee, D. P. Nicolella, B. R. Furman, S. Wellinghoff, and R. Rawls, "Improving fracture toughness of dental nanocomposites by interface engineering and micromechanics," *Engineering Fracture Mechanics,* vol. 74, pp. 1857-1871, Aug 2007.

[23] K. A. Athanasiou, C. F. Zhu, D. R. Lanctot, C. M. Agrawal, and X. Wang, "Fundamentals of biomechanics in tissue engineering of bone," *Tissue Engineering,* vol. 6, pp. 361-381, 2000.

[24] M. M. Tunney, A. J. Brady, F. Buchanan, C. Newe, and N. J. Dunne, "Incorporation of chitosan in acrylic bone cement: Effect on antibiotic release, bacterial biofilm formation and mechanical properties," in *Special Section: Selected Papers from the 21st European Conference on Biomaterials, Brighton, UK, 9-13 September 2007. Guest Editors: Andrew Lloyd and*

Matteo Santin, Van Godewijckstraat 30, Dordrecht, 3311 GZ, Netherlands, 2008, pp. 1609-1615.

Morshed P.H. Khandaker has been serving as an assistant professor in the department of Engineering & Physics at University of Central Oklahoma since Fall 2008. He received Ph.D. in mechanical engineering from Texas Tech University, Lubbock, in August, 2007. From 2004-2007, he had been serving as an instructor in the department of mechanical engineering at Texas Tech University. He is active and interested in conducting research in design, fracture and failure modeling, and material characterization of biomechanical systems. He is teaching in the area of solid mechanics, material science, mechanical design, machine dynamics, vibration, and computational mechanics.

Stefano Tarantini received BSc in biomedical engineering from University of Central Oklahoma, Edmond, in May, 2012. He is currently pursuing graduate study in biomedical science from Fall 2012 at University of Oklahoma Health Science Center. He is active and interested in conducting research in biomechanics, cell mechanics, tissue engineering, and material characterization of biomechanical systems.